

Letter to the Editor
Maximum-entropy maps of the Be shell star ζ Tauri from optical long-baseline interferometry
A. Quirrenbach^{1,2,3}, D.F. Buscher^{1,2}, D. Mozurkewich^{1,4}, C.A. Hummel^{1,2}, and J.T. Armstrong^{1,2}
¹ NRL/USNO Optical Interferometer Project; U.S. Naval Observatory, AD5; 3450 Mass. Ave., NW; Washington, DC 20392-5420, USA

² Universities Space Research Association (USRA); 300 D Street, SW, Suite 801; Washington, DC 20024, USA

³ Present address: MPI für Extraterrestrische Physik, Postfach 1603, D-85748 Garching bei München, Germany

⁴ Remote Sensing Division, Naval Research Laboratory, Code 7215; Washington, DC 20375, USA

Received 9 December 1993 / Accepted 13 January 1994

Abstract. We present the first maximum-entropy maps reconstructed from visibility amplitudes obtained with an optical long-baseline interferometer. They show the Be shell star ζ Tauri. In the continuum at 550 nm the star is an unresolved point source, whereas in the light of the $H\alpha$ line an extended, elongated structure is observed. The best-fit parameters of an elliptical Gaussian model are: major axis $a = 3.55 \pm 0.33$ mas, axial ratio $r = 0.30 \pm 0.03$, position angle $\phi = -59^\circ \pm 4^\circ$. The morphology of the $H\alpha$ emission region is most easily interpreted as a disk seen almost edge-on; if this disk is axially symmetric, a limit for the inclination $i \geq 73^\circ$ can be derived. Our observations provide further evidence for the equatorial disk model of Be stars.

Key words: Techniques: interferometric – Stars: emission line, Be – Stars: imaging – Stars: individual: ζ Tau – Stars: mass-loss

1. Introduction

While stellar long-baseline interferometry has become a very successful tool to measure stellar diameters (e.g. Mozurkewich et al. 1991) and to determine “visual” orbits of close binaries (e.g. Armstrong 1992), extraction of more detailed information about the stellar brightness distribution from the visibility data remains a considerable challenge. The first notable achievement in this area was the measurement of Sirius’ limb darkening by Hanbury Brown et al. (1974) with the Narrabri intensity interferometer. Possible structure in β Andromedae was inferred from I2T data at 1.65 and 2.2 μm by Di Benedetto and Bonneau (1990). Observations with the MkIII interferometer have shown that Mira’s atmosphere is strongly asymmetric and changes shape on the timescale of months (Quirrenbach et al. 1992). The $H\alpha$ emission region of the Be star γ Cassiopeiae has been observed with the I2T (Thom et al. 1986), GI2T (Mourard et al. 1989), and MkIII (Quirrenbach et al. 1993) instruments; the results support the long-standing picture of a rotating disk-shaped envelope.

Send offprint requests to: A. Quirrenbach (Garching address)

Whereas the interpretation of these data sets has been based on fitting models with a small number of free parameters to the measured visibilities, future interferometric arrays will rely on methods similar to those currently used in radio interferometry to reconstruct the sky brightness distribution. These algorithms have already been adapted for the analysis of data obtained with aperture masks on large telescopes (Haniff et al. 1988, Buscher et al. 1990). Closure phase information will be crucial to obtain images with high fidelity and dynamic range using instruments such as the Big Optical Array¹ (BOA), the ESO Very Large Telescope Interferometer (VLTI) and the Cambridge Optical Aperture Synthesis Telescope (COAST). It is possible, however, to obtain images of simple objects from amplitude data only. Here we present a maximum-entropy reconstruction of the $H\alpha$ disk of the Be shell star ζ Tauri from data obtained with the MkIII Optical Interferometer.

2. The observations

ζ Tauri (B4 IIIe, $m_V = 3.0$) was observed with the MkIII instrument² on 12 nights between Sept. 27 and Nov. 30, 1992; some test observations had been performed on Dec. 27, 1991, and Jan. 01, 1992. The MkIII is a Michelson interferometer with a single north-south baseline, whose length can be varied between 3.0 and 31.5 m. In addition to the wide-band channel used for active fringe-tracking, three data channels are available; their bandpasses are defined by interference filters. Automatic acquisition of the stellar images and of the fringes under computer control allows for rapid switching between different stars, so that observations of the program stars can be sandwiched between calibrators with known diameters. With this observing strategy, an accurate calibration of the system visibility (i.e., the fringe contrast obtained on a point source), can be achieved as a function of seeing, zenith angle, and time. Detailed descriptions of the instrument and observing procedures are given by Shao et al. (1988) and Mozurkewich et al. (1991).

¹The BOA is the imaging portion of the Navy Prototype Optical Interferometer under construction at Lowell Observatory.

²The MkIII Optical Interferometer on Mt. Wilson near Los Angeles, CA, is operated by the Remote Sensing Division of the Naval Research Laboratory (NRL).

Report Documentation Page

Form Approved
OMB No. 0704-0188

Public reporting burden for the collection of information is estimated to average 1 hour per response, including the time for reviewing instructions, searching existing data sources, gathering and maintaining the data needed, and completing and reviewing the collection of information. Send comments regarding this burden estimate or any other aspect of this collection of information, including suggestions for reducing this burden, to Washington Headquarters Services, Directorate for Information Operations and Reports, 1215 Jefferson Davis Highway, Suite 1204, Arlington VA 22202-4302. Respondents should be aware that notwithstanding any other provision of law, no person shall be subject to a penalty for failing to comply with a collection of information if it does not display a currently valid OMB control number.

1. REPORT DATE 13 JAN 1994	2. REPORT TYPE	3. DATES COVERED 00-00-2011 to 00-00-2011			
4. TITLE AND SUBTITLE Maximum-entropy Maps Of The Be Shell Star Zeta Tauri From Optical Long-Baseline Interferometry		5a. CONTRACT NUMBER			
		5b. GRANT NUMBER			
		5c. PROGRAM ELEMENT NUMBER			
6. AUTHOR(S)		5d. PROJECT NUMBER			
		5e. TASK NUMBER			
		5f. WORK UNIT NUMBER			
7. PERFORMING ORGANIZATION NAME(S) AND ADDRESS(ES) U. S. Naval Observatory, 3450 Mass Ave., N.W., Washington, DC, 20392		8. PERFORMING ORGANIZATION REPORT NUMBER			
9. SPONSORING/MONITORING AGENCY NAME(S) AND ADDRESS(ES)		10. SPONSOR/MONITOR'S ACRONYM(S)			
		11. SPONSOR/MONITOR'S REPORT NUMBER(S)			
12. DISTRIBUTION/AVAILABILITY STATEMENT Approved for public release; distribution unlimited					
13. SUPPLEMENTARY NOTES Astronomy and Astrophysics, vol. 283, no. 2, p. L13-L16					
14. ABSTRACT We present the first maximum-entropy maps reconstructed from visibility amplitudes obtained with an optical long-baseline interferometer. They show the Be shell star zeta Tauri. In the continuum at 550 nm the star is an unresolved point source, whereas in the light of the H-alpha line an extended, elongated structure is observed. The best-fit parameters of an elliptical Gaussian model are: major axis a = 3.55 +/- 0.33 mas, axial ratio r = 0.30 +/- 0.03, position angle phi = -59 deg +/- 4 deg. The morphology of the H-alpha emission region is most easily interpreted as a disk seen almost edge-on; if this disk is axially symmetric, a limit for the inclination i greater than or equal to 73 deg can be derived. Our observations provide further evidence for the equatorial disk model of Be stars.					
15. SUBJECT TERMS					
16. SECURITY CLASSIFICATION OF:			17. LIMITATION OF ABSTRACT Same as Report (SAR)	18. NUMBER OF PAGES 13	19a. NAME OF RESPONSIBLE PERSON
a. REPORT unclassified	b. ABSTRACT unclassified	c. THIS PAGE unclassified			

For the observations reported here, we used baselines ranging from 4.2 to 31.5 m. The main data channel was centered on the $H\alpha$ line at 656 nm and had a width of 1 nm. A second channel at the same central wavelength, but 10 nm wide, was used for control purposes; this is necessary because the 1 nm wide filter tends to attenuate the wings of the rather wide $H\alpha$ line. The third channel was centered at 550 nm and 25 nm wide; it was used to measure the stellar continuum for comparison. Each individual observation (“scan”) was 300 s long; this gave sufficient signal-to-noise on the program as well as calibrator stars in all channels. The observations were scheduled in a way that would optimize the hour-angle coverage on the longer baselines; the resulting coverage of the Fourier (uv) plane for the combined data on ζ Tauri from all nights in the narrow $H\alpha$ channel is shown in Fig. 1.

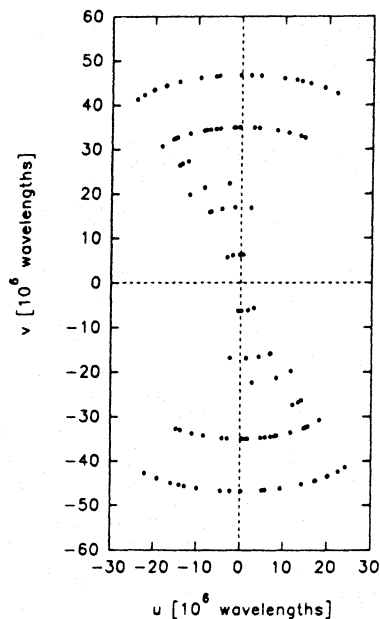


Fig. 1. Coverage of the Fourier (uv) plane, for the data in the $H\alpha$ channel.

3. Maximum-entropy mapping

The MkIII standard data reduction software incoherently integrates the square of the visibility amplitude V_{raw}^2 estimated from each 4 ms sample over the length of the scan, and divides it by the system visibility, giving V_{cal}^2 . The calibrated data can then be used by model fitting or image reconstruction programs similar to those used in radio interferometry. For the analysis of the ζ Tauri data, we used an iterative maximum-entropy algorithm, which seeks to find the “smoothest” image which is compatible with the data. In each step, it calculates model visibilities from a test image, compares them to the data and computes χ_{red}^2 and its partial derivatives, and modifies the image along the direction of the gradient of $\chi_{\text{red}}^2 - \lambda S$, where χ_{red}^2 is the reduced χ^2 , λ a Lagrange multiplier, and S the image entropy (see e.g. Narayan and Nitayanda 1984). Starting from a user-specified initial image (typically a point source at the origin on a low uniform background), the algorithm thus tries to converge to the image which has $\chi_{\text{red}}^2 = 1$ and maximum entropy. More detailed descriptions of the algorithm are given by Skilling and Bryan (1984) and Buscher (1993).

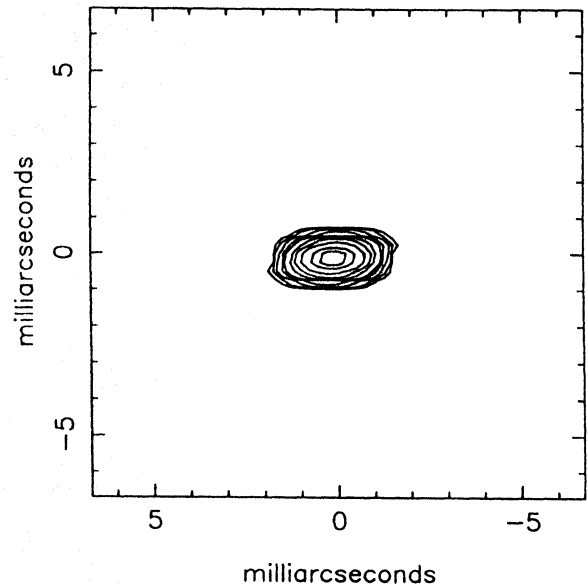


Fig. 2. Maximum-entropy reconstruction of ζ Tauri in the continuum channel centered at 550 nm. Contour levels are 0.1, 0.2, 0.5, 1, 2, 5, 10, 20, 50, and 80% of the peak.

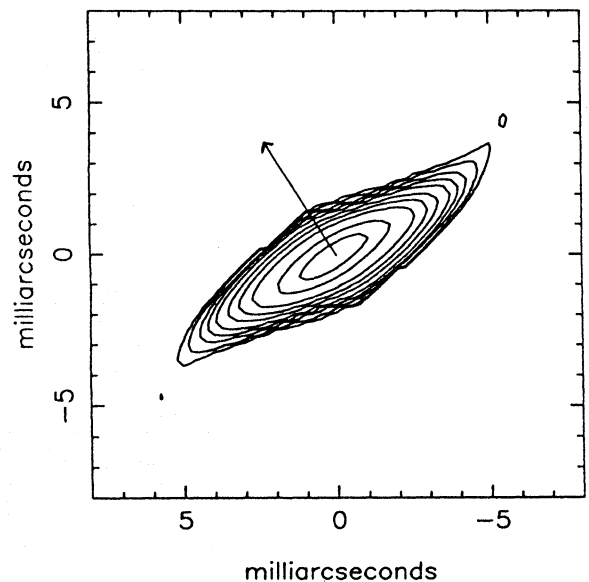


Fig. 3. Maximum-entropy reconstruction of ζ Tauri in the $H\alpha$ emission line (656 nm). Contour levels are as in Fig. 2. The arrow indicates the position angle of the linear polarization.

We tested the program using one night’s data on the binary star Capella (α Aurigae); it converged to an image with two pointlike stars at a separation and position angle in agreement with results from model fitting and from a new improved orbital solution (Hummel et al. 1994). During these tests we found that the convergence was substantially improved and the sidelobe level in the final image drastically reduced when V^2 at zero spacing was explicitly set to 1. In principle, this effect is well-known in radio astronomical applications, but there the flux density at zero spacing is frequently not known precisely enough to aid the maximum-entropy algorithm significantly.

The photosphere of ζ Tauri is expected to be almost un-

resolved even on our longest baseline; estimates for the stellar angular diameter, based on photometric data, range from 0.4 mas (Ochsenbein and Halbwachs 1982) to 0.6 mas (Glushneva 1987). Our data in the 550 nm channel show indeed only marginal indications of resolution; on the 31.5 m baseline $V^2 \approx 0.8$. This allows us to set an upper limit of ≈ 1 mas on the size of the photosphere. Based on radial velocity variations of the shell lines it has been argued that ζ Tauri is in a binary system with period 132.91 days (Delplace and Chambon 1976). Since there is no signature of the secondary in our 550 nm data, we can set a limit on the magnitude difference $\Delta m_V \geq 2.5$ (unless the separation $d \geq 100$ mas, which is incompatible with the total mass, period and distance of the system). This is consistent with the finding by Floquet et al. (1989) that the presumed secondary cannot be a bright (luminosity class II) giant, which would fill its Roche lobe.

In Fig. 2, we present the maximum-entropy map of ζ Tauri at 550 nm. This map is basically the point-source response corresponding to our uv coverage; the apparent elongation in E-W direction is due to the fact that the resolution is substantially better in the N-S than in E-W direction (see Fig. 1).

In the light of the $H\alpha$ line, ζ Tauri is clearly resolved and strongly elongated (in the projection onto the sky). Figure 3 shows the maximum-entropy map from the data taken in the 1 nm wide channel. The fit to the data is excellent, as can be seen in Fig. 4, where we superpose the model prediction on the data obtained on the longest (31.5 m) baseline. (The baseline position angle is the angle of the corresponding point in the uv plane, measured clockwise from the v axis.) It should be pointed out that the strong elongation of the $H\alpha$ emission region is apparent directly from the visibility data: a spherically symmetric object would give visibilities that are symmetric with respect to meridian transit (baseline position angle 0°).

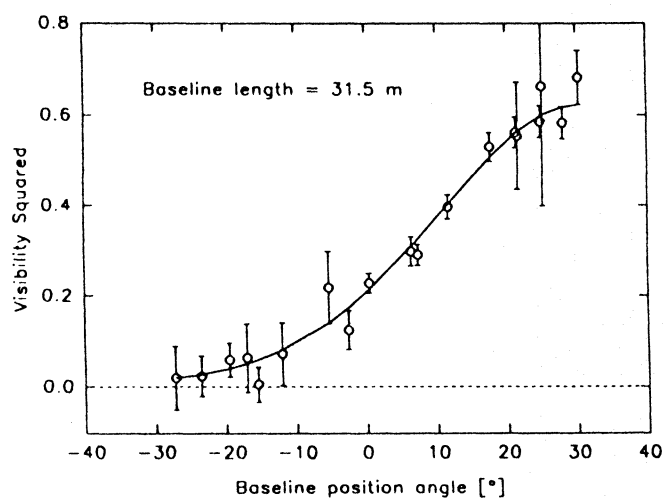


Fig. 4. Visibility data in the 1 nm wide $H\alpha$ channel from the longest (31.5 m) baseline, and maximum-entropy model.

We have performed a series of tests with a number of different starting models to verify that the maximum-entropy algorithm converged consistently to basically identical solutions. Nevertheless, it should be borne in mind that a maximum-

entropy “image” is nothing but a model representation for the data and thus susceptible to a number of artifacts.

First, the lack of phase information in our data will tend to favor a mirror-symmetric reconstruction. Our test with a reconstruction of the binary star Capella, which did not give a “ghost image” of the secondary, shows that this is not necessarily the case, however. If the object is fairly simple, amplitude data with sufficient signal-to-noise can produce asymmetric reconstructions. In the case of ζ Tauri we cannot decide whether the structure of the envelope is indeed symmetric or whether the signal-to-noise in the data is not high enough to make the maximum-entropy program converge to an asymmetric solution. Rapid variations of the emission line profiles (e.g. Yang et al. 1990) suggest that the $H\alpha$ emitting region might be either asymmetric or not centered on the star (Telting et al. 1993). On the other hand, Thom et al. (1986) find that the envelope of γ Cassiopeiae is in fact symmetric and centered on the star to within 0.3 mas. Future interferometric observations with longer baselines and high-quality phase information are needed to decide this question.

Second, the asymmetric coverage of the uv plane will show up as an artificial elongation of the contour lines in E-W direction, as discussed above. The continuum map in Fig. 2 can be used as a reference for the point-source response. It should be pointed out that maximum-entropy maps do not have a defined “beam shape”. (To facilitate the comparison, the reproductions of the two maps have been scaled by the wavelength ratio.)

To derive numerical parameters for the $H\alpha$ emission region, we have therefore also fitted a simple elliptical Gaussian model to the visibility data. The best-fit parameters of this model are: major axis $a = 3.55 \pm 0.33$ mas, axial ratio $r = 0.30 \pm 0.03$, position angle $\phi = -59^\circ \pm 4^\circ$ (measured from north through east). The quoted errors are formal errors obtained from the increase of χ^2 when the parameters are varied; the value for r might actually be smaller, since the size of the minor axis is very close to our resolution limit. This elliptical model gives a very good representation of the overall appearance of the maximum entropy map.

The total extent of the $H\alpha$ emission region is ≈ 10 mas (3 FWHM of the Gaussian model, see also Fig. 3), or about 15 photospheric diameters. This value agrees roughly with model predictions (e.g. Poeckert and Marlborough 1978).

4. Discussion

The observed axial ratio of the $H\alpha$ emission region $r = 0.30$ implies that the intrinsic geometry is strongly non-spherical. This result is inconsistent with nearly spherical models for Be stars (e.g. Doazan 1987) and provides additional evidence for a disklike structure. Both fairly thick (opening angle $\sim 15^\circ$, Poeckert and Marlborough 1978) and very thin (opening angle $\sim 0.5^\circ$, Bjorkman and Cassinelli 1993) disks are consistent with our data; in the latter model it might be difficult to explain the strong shell absorption, however.

Under the assumption that the disk is axially symmetric, a lower limit to the inclination of the axis $i \geq \arccos 0.30 = 73^\circ$ is derived from a simple geometric consideration. The high intrinsic degree of polarization (Poeckert et al. 1979, McDavid 1990) provides independent, although less direct, evidence for a large inclination of ζ Tauri. Published values for $v \sin i$ range from 220 km s^{-1} (Slettebak 1982) to 320 km s^{-1} (Uesugi and Fukuda 1982), but the upper end of this range seems to be

preferred (Yang et al. 1990). Gao and Cao (1986) have tried to determine the inclination of ζ Tauri using a method proposed by Hutchings (1976), which is based on the comparison of optical and UV line widths; they found $i \approx 60^\circ$. Combining these values for $v \sin i$ and i leads to conclusion that the rotation rate of ζ Tauri is very close to the critical value, $\omega/\omega_{\text{crit}} = 1$ (Ruusalepp 1989). The larger inclination indicated by our data gives $\omega/\omega_{\text{crit}} \approx 0.85$, however, supporting the idea that Be stars do not rotate at the critical velocity. Our limit for the inclination is also consistent with the supposition that Be stars with shell absorption lines in the visible part of the spectrum are seen almost equator-on (e.g. Slettebak 1979).

The continuum polarization of Be stars is believed to be due to scattering by free electrons in the circumstellar disk (McLean 1979). This explanation predicts that the polarization position angle χ should be perpendicular to the equatorial plane. Poeckert et al. (1979) and McDavid (1990) find $\chi \approx 33^\circ$; with only a small interstellar contribution. The position angle $\phi = -59^\circ \pm 4^\circ$ from our data is indeed perpendicular to χ .

5. Conclusions

For the first time, we have been able to reconstruct a maximum-entropy map from visibility amplitudes obtained with optical long-baseline interferometry. This represents an important step towards routine imaging with milliarcsecond resolution, the declared goal of the interferometric arrays currently under construction.

Our maximum-entropy map of ζ Tauri in the $H\alpha$ line should be interpreted with some caution, because of the lack of phase information and the non-uniform coverage of the uv plane. Nevertheless, it confirms several predictions of the equatorial disk model for Be stars. While elongated structures have been observed for the radio emission of ψ Persei (Dougherty and Taylor 1992) and for the $H\alpha$ emission of γ Cassiopeiae (Quirrenbach et al. 1993), the observed axial ratio is more extreme for ζ Tauri. This allows tighter constraints to be placed on the intrinsic geometry; a meaningful lower limit to the inclination can be derived under the assumption of axial symmetry.

Future observations with longer baselines and improved uv coverage will give valuable additional information about the shape and structure of Be star disks. The emission line regions of these and similar objects are particularly good targets of optical long-baseline arrays. The small central star can be used as a reference object for fringe tracking, and the line-continuum phase difference can be used directly for imaging; phase closure methods are not needed. This gives a large increase in phase information for arrays with a small number of elements. Furthermore, even data with moderate signal-to-noise will carry valuable astrophysical information. (In contrast, the main goal of the BOA, namely imaging of stellar photospheres, requires extremely high signal-to-noise and excellent calibration to detect small deviations from simple uniform or limb-darkened disk models.) Finally, a simple estimate shows that the BOA will be sensitive enough to put ~ 10 spectral channels across the $H\alpha$ line. A combination of the approaches taken by Mourard et al. (1989) and in this work will thus make detailed studies of the kinematics of Be star disks possible.

Acknowledgements. We thank C.S. Denison and L.W. Rarogiewicz for their help with the data acquisition. A. Quirrenbach acknowledges support by a Feodor Lynen Fellowship from the

Alexander von Humboldt Foundation. Basic research in Infrared and Optical Interferometry at NRL is supported by the Office of Naval Research through funding document number N00014-93-WX-35012, under NRL work unit 1798. The maximum entropy program uses the MEMSYS2 algorithm from Maximum Entropy Data Consultants, Ltd. We have made use of the Simbad database, operated at CDS, Strasbourg, France.

References

- Armstrong, J.T., 1992, in *IAU Coll. 135, Complementary Approaches to Double and Multiple Star Research*, ed. H.A. McAlister and W.I. Hartkopf, ASP Conf. Ser. 32, p. 492
- Bjorkman, J.E., Cassinelli, J.P., 1993, *ApJ* 409, 429
- Buscher, D.F., 1993, in *IAU Symp. 158, Very High Angular Resolution Imaging*, ed. J.G. Robertson and W.J. Tango, Kluwer, in press
- Buscher, D.F., Haniff, C.A., Baldwin, J.E., Warner, P.J., 1990, *MNRAS* 245, 7P
- Delplace, A.M., Chambon, M.Th., 1976, in *IAU Coll. 70, Be and Shell Stars*, ed. A. Slettebak, Reidel, Dordrecht, p. 79
- Di Benedetto, G.P., Bonneau, D., 1990, *ApJ* 358, 617
- Doazan, V., 1987, in *IAU Coll. 92, Physics of Be Stars*, ed. A. Slettebak and T.P. Snow, Cambridge Univ. Press, p. 384
- Dougherty, S.M., Taylor, A.R., 1992, *Nature* 359, 808
- Floquet, M., Hubert, A.M., Maillard, J.P., Chauville, J., Chatzichristou, H., 1989, *A&A* 214, 295
- Gao, W., Cao, H., 1986, *Acta Astrophys. Sin.* 6, 143
- Glushneva, I.N., 1987, *AZh* 64, 601
- Hanbury Brown, R., Davis, J., Lake, R.J.W., Thompson, R.J., 1974, *MNRAS* 167, 475
- Haniff, C.A., Mackay, C.D., Titterton, D.J., Sivia, D., Baldwin, J.E., Warner, P.J., 1988, *Nat* 328, 694
- Hummel, C.A., et al., 1994, *AJ*, submitted
- Hutchings, J.B., 1976, *PASP* 88, 5
- McDavid, D., 1990, *PASP* 102, 773
- McLean, I.S., 1979, *MNRAS* 186, 265
- Mourard, D., Bosc, I., Labeyrie, A., Koechlin, L., Saha, S., 1989, *Nature* 342, 520
- Mozurkewich, D., Johnston, K.J., Simon, R.S., et al., 1991, *AJ* 101, 2207
- Narayan, R., Nitnayanda, R., 1984, *ARA&A* 24, 127
- Ochsenbein, F., Halbwegs, J.L., 1982, *A&AS* 47, 523
- Poeckert, R., Bastien, P., Landstreet, J.D., 1979, *AJ* 84, 812
- Poeckert, R., Marlborough, J.M., 1978, *ApJ* 220, 940
- Quirrenbach, A., Mozurkewich, D., Armstrong, J.T., Johnston, K.J., Colavita, M.M., and Shao, M. 1992, *A&A* 259, L19
- Quirrenbach, A., Hummel, C.A., Buscher, D.F., Armstrong, J.T., Mozurkewich, D., Elias, N.M., 1993, *ApJ* 416, L25
- Ruusalepp, M. 1989, *Tartu Astroph. Obs. Teated*, No. 100, 1
- Shao, M., Colavita, M.M., Hines, B.E., et al., 1988, *A&A* 193, 357
- Skilling, J., Bryan, R.K., 1984, *MNRAS* 211, 111
- Slettebak, A., 1979, *Space Sci. Rev.* 23, 541
- Slettebak, A., 1982, *ApJS* 50, 55
- Telting, J.H., Waters, L.B.F.M., Persi, P., Dunlop, S.R., 1993, *A&A* 270, 355
- Thom, C., Granes, P., Vakili, F., 1986, *A&A* 165, L13
- Uesugi, A., Fukuda, I., 1982, *Revised Catalogue of Stellar Rotational Velocities*, Kyoto University, Kyoto, Japan
- Yang, S., Walker, G.A.H., Hill, G.M., Harmanec, P., 1990, *ApJS* 74, 595